J Appl Physiol 94: 1602–1618, 2003.
First published November 8, 2002; 10.1152/japplphysiol.00281.2002.

A model for integrative study of human gastric acid secretion

Ian M. P. Joseph,[1] Yana Zavros,[2] Juanita L. Merchant,[2] and Denise Kirschner[1]
Departments of [1]Microbiology and Immunology and [2]Internal Medicine, The University of Michigan Medical School, Ann Arbor, Michigan 48109

Submitted 2 April 2002; accepted in final form 4 November 2002

Joseph, Ian M. P., Yana Zavros, Juanita L. Merchant, and Denise Kirschner. A model for integrative study of human gastric acid secretion. *J Appl Physiol* 94: 1602–1618, 2003. First published November 8, 2002; 10.1152/japplphysiol.00281.2002.—We have developed a unique virtual human model of gastric acid secretion and its regulation in which food provides a driving force. Food stimulus triggers neural activity in central and enteric nervous systems and G cells to release gastrin, a critical stimulatory hormone. Gastrin stimulates enterochromaffin-like cells to release histamine, which, together with acetylcholine, stimulates acid secretion from parietal cells. Secretion of somatostatin from antral and corpus D cells comprises a negative-feedback loop. We demonstrate that although acid levels are most sensitive to food and nervous system inputs, somatostatin-associated interactions are also important in governing acidity. The importance of gastrin in acid secretion is greatest at the level of transport between the antral and corpus regions. Our model can be applied to study conditions that are not yet experimentally reproducible. For example, we are able to preferentially deplete antral or corpus somatostatin. Depletion of antral somatostatin exhibits a more significant elevation of acid release than depletion of corpus somatostatin. This increase in acid release is likely due to elevated gastrin levels. Prolonged hypergastrinemia has significant effects in the long term (5 days) by promoting enterochromaffin-like cell overgrowth. Our results may be useful in the design of therapeutic strategies for acid secretory dysfunctions such as hyper- and hypochlorhydria.

gastrin; stomach; mathematical model; somatostatin; histamine

ACID SECRETION FROM PARIETAL cells in the stomach is a highly regulated, complex, and dynamic process optimized to facilitate food digestion. Not only are there interactions between the central and enteric nervous systems (CNS and ENS, respectively), but a complex network of paracrine and endocrine cells is also involved. The overall goal is maintenance of stomach luminal pH within a strict range (i.e., pH homeostasis); food consumption and other deviations altering this range increase or decrease acid release.

Four cell populations and their secreted products form the core acid secretory process in humans. These four cell populations are gastrin (G)- and somatostatin (D)-secreting cells, enterochromaffin-like (ECL) cells, and parietal cells. G and ECL cell products stimulate acid secretion (positive feedback); D cells inhibit acid release (negative feedback). Inconsistencies in the integration of the feedback loops exist and may be due to species-specific differences. For example, the ability of gastrin to directly stimulate acid release in some species is in dispute (5, 96). Other inconsistencies involving effector and acid regulation may relate to the experimental approach, such as in vitro vs. in vivo studies. The basic requirement for acid secretion, however, appears to be conserved among the species (22, 61). The need for an integrative approach to study gastric acid secretion is clear. Mathematical modeling is a powerful tool that allows for exploration of the integrated system and its components in a systematic fashion. Furthermore, mathematical modeling is immune to inconsistencies that often arise from comparison of in vivo and in vitro studies.

Mathematical models based on acid secretion have appeared in the literature (17, 20, 58). De Beus et al. (17) explored the coupling of gastric acid release to bicarbonate secretion through extensive mathematical analyses of the cascade of molecular and ionic events constituting acid secretion. Licko and Ekblad (58) focused on gastric acid as a two-step, sequential process. They modeled formation of acid that contributes to an acid storage pool and translocation of stored acid into the lumen of the stomach. Both models provide insight into acid secretion but do not address regulation of acid secretion.

In this study, we use a novel mathematical model to describe the complex system of gastric acid regulation. Our model is unique, because we consider regulatory processes that have been identified experimentally as essential for proper maintenance of acid secretion. Our two main goals are to validate the model and perform new experiments. Validation involves comparing simulations during healthy and depletion situations with experimental data. The model can then be used to perform studies not yet experimentally reproducible. For example, we are able to preferentially deplete antral or corpus somatostatin.

METHODS

The stomach consists of many histologically distinct regions (Fig. 1*A*); however, we simplify the model by describing

Address for reprint requests and other correspondence: D. Kirschner, 6730 Medical Sciences Bldg. II, The University of Michigan, Ann Arbor MI 48109-0620 (E-mail: kirschne@umich.edu).

The costs of publication of this article were defrayed in part by the payment of page charges. The article must therefore be hereby marked "*advertisement*" in accordance with 18 U.S.C. Section 1734 solely to indicate this fact.

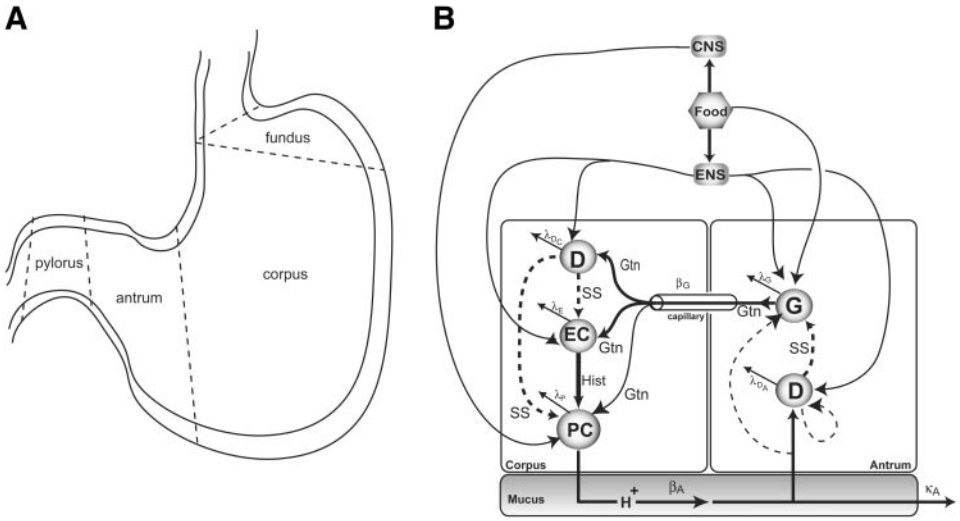

Fig. 1. *A*: histology of the stomach. *B*: model diagram of effector regulation of gastric acid secretion. Model includes positive and negative effector feedback systems. Cells are assigned to their respective compartments. G cells in the antrum secrete gastrin (Gtn), an effector of gastric acid secretion. Gtn not only stimulates histamine (Hist) release from enterochromaffin-like (ECL) cells (EC) and gastric acid (H^+) secretion from parietal cells (PC) but also stimulates somatostatin (SS) secretion. Greek symbols represent rates at which events occur: β, transport rate; λ, death rate; κ_A, washout rate of acid with gastric emptying. Also shown are central and enteric neural stimuli (CNS and ENS, respectively) supplied to the physiological system on feeding. Solid arrows, positive stimuli; dashed arrows, negative stimuli. Weight of arrows indicates relative intensity of stimulus.

two main compartments: the antrum and corpus regions (Fig. 1*B*). The relevant biological processes affecting acid secretion occur here and include dynamic changes in cell populations; secretion of effectors, neurotransmitters, and acid; and release of gastric protective factors. We outline the components of the model and our assumptions; the mathematical details are described in the APPENDIX.

Model

Cellular elements. The key cells involved in the model are found in gastric glands of the antrum and corpus (Fig. 2). Several studies have outlined gastric paracrine, endocrine, and exocrine cell development (40–47). These electron microscopy studies show that the lineage of these differentiated cells can be traced to undifferentiated stem cells abundant in the isthmus of gastric glands (41). Cells arising from stem cells are terminally differentiated and, with the exception of ECL cells, do not undergo mitosis (102, 103). We monitor seven cell populations in our model (Fig. 3): antral and corpus stem cells, antral G cells, antral and corpus D cells, ECL cells, and corpus parietal cells.

Although cell fluctuations are minimal in the short term (24 h), they have been observed in the long term (5 days). For example, during prolonged hypergastrinemia, ECL cell overgrowth results in increased acid secretion. We use a 5-day period and show that it is sufficient for detection of significant cell changes. These changes may ultimately affect gastric function; therefore, it is necessary to track cell dynamics in our model (1, 48). Under normal conditions, we assume that stem cell differentiation balances the loss of differentiated cells, resulting in cell homeostasis. We also assume that differentiation is not a random event but is governed by feedback mechanisms. Without these mechanisms, differentiation would be uncontrolled, leading to exacerbated G, D, ECL, and parietal cell populations. Although feedback mechanisms controlling stem cell differentiation have not been characterized in the stomach, their existence has been demonstrated in nongastric systems (70). In addition to feedback mechanisms, other factors may also influence stem cell differentiation, such as long-term presence or absence of food and prolonged neutral pH conditions in the stomach, such as during chronic hypochlorhydria (2, 4, 8, 93). Standard loss of G, D, ECL, and parietal cells occurs through apoptosis, sloughing of mucosal lining, or engulfment by neighboring cells (19, 40, 43, 46). We assume equivalent loss rates for cells in the same region (antrum or corpus).

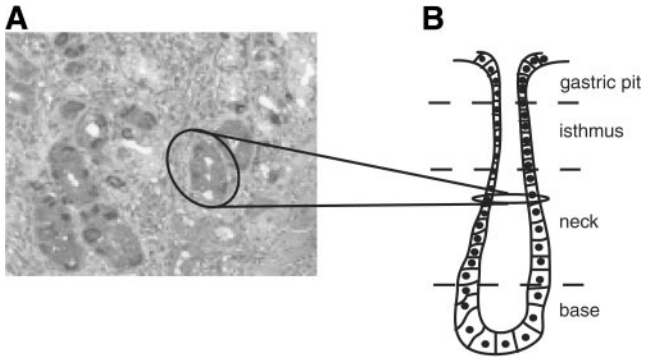

Fig. 2. Cross-sectional and schematic longitudinal section of a gastric gland. *A*: stained parietal cells in corpus region of a human stomach. Ellipse highlights a cross-sectional view of a typical corpus gland. *B*: schematic view of longitudinal section of a gastric gland; cross-sectional view fails to capture 3-dimensional nature of gland. It is assumed that the human gland is long and tubular. However, species-specific variations occur in arrangements of glands.

Feeding function. We model a standard American diet of three meals a day (at 0600, 1200, and 1800) using a sinusoidal function to describe the volume of food consumed (Fig. 4). The volume of food increases with each successive meal during the day and ranges between 0.0 and 1.0 liter, with 1.5 liters being the maximal capacity of the stomach. We rigorously test the model with other feeding functions in which the feeding intervals are varied (data not shown). The response is appropriate: there is strong correlation between the modality pattern of the feeding function and the effector, bicarbonate, and acid responses. This is critical for optimal food digestion.

Food also buffers acid and increases luminal pH. We assume that buffering of acid is dependent on food volume. We assume that there is an upper limit on the buffering capacity of food. Michaelis-Menten dynamics adequately describe this effect.

Neural elements. ENS and CNS neurotransmitters are secreted in response to food volume. There is a lack of kinetic data describing the influence of food volume on neural activity; we assume that neural activity increases in a Michaelis-Menten manner with food volume. Neuropeptides are metabolically degraded, and this degradation is governed by first-order kinetics (see APPENDIX). Food stimulates CNS activity, which is conducted via the vagus nerve to the ENS of the stomach, resulting in acid and gastrin release (16). Indirect

action of the CNS on acid secretion has also been demonstrated; cholinergic neurotransmitters inhibit somatostatin secretion, promoting acid release (16, 73, 91). The physical (degree of distension) and biochemical (pH, neural, and effector concentrations) states of the stomach then feed back to the CNS, modulating its response (94, 95) (Fig. 1*B*).

The mechanism whereby the CNS controls the ENS is not fully understood (11); however, for modeling purposes, we assume that the two are independent. This does not have any qualitative effect on our results (data not shown).

Effector regulation of acid secretion. When food enters the lumen, alterations in stomach pH and volume, together with neural stimulation, lead to acid secretion. G cells within the antrum secrete gastrin, which is released into antral blood capillaries and diffuses into the corpus (Fig. 1*B*). In the corpus, gastrin directly stimulates parietal cells to secrete gastric acid (107) and stimulates ECL cells to release histamine in conjunction with ENS neurotransmitters (48, 82). Histamine acts in a paracrine manner in conjunction with gastrin and acetylcholine, enhancing acid secretion (16, 59), and also potentiates gastrin stimulation of parietal cells (96). To downregulate these processes in the antrum and corpus, D cells secrete somatostatin, a negative effector of gastric acid secretion (14, 63, 92). Gastrin, somatostatin, and histamine are released in a dose-dependent manner on appropriate stimulation (7, 54, 67). In addition to effectors described above, gastric acid secretion by parietal cells can also be directly stimulated by CNS activity in response to food, although not to the same extent (72).

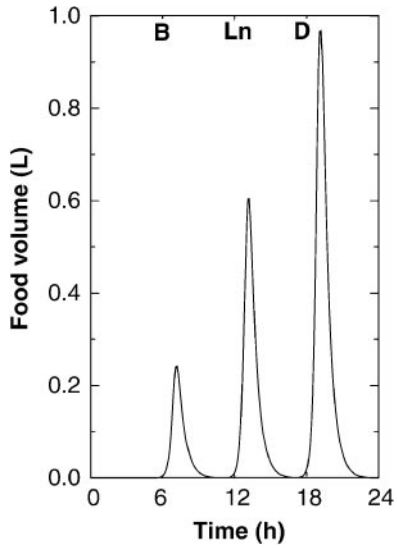

Fig. 4. Food input to virtual human gastric system. B, Ln, and D, breakfast (0700), lunch (1300), and dinner (1900), respectively. Amplitude of peak at each meal represents volume of food intake.

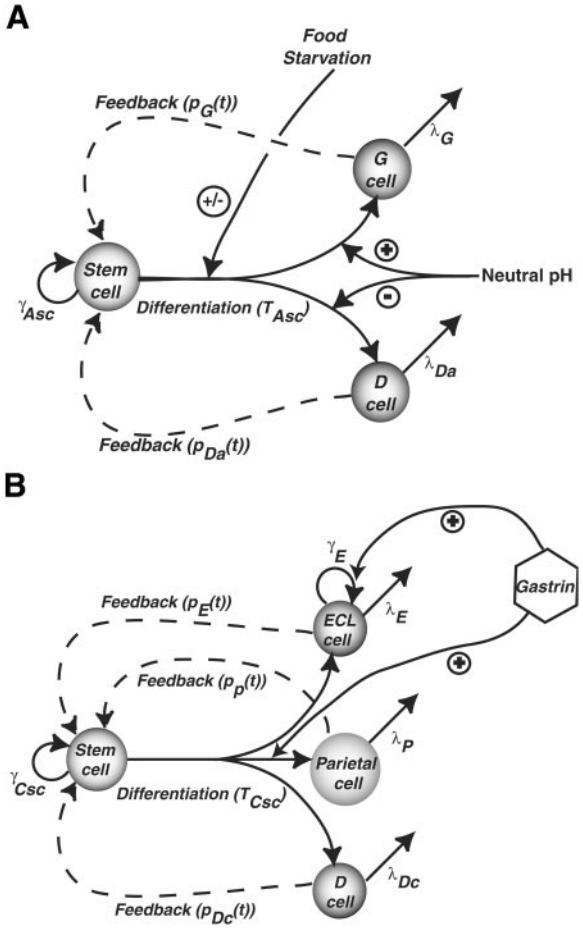

Fig. 3. Ontogeny of G, D, ECL, and parietal cells from underlying antral (Asc) and corpus (Csc) stem cells. *A*: differentiation within antrum. *B*: differentiation in corpus region. Dashed lines, feedback control of stem cell differentiation [$p(t)$]. Alphanumeric and Greek symbols represent rates at which respective processes occur: γ and λ, growth and death rates; T, differentiation of respective stem cells.

There is a morphological and functional dissimilarity between antral and corpus D cells (35). Antral D cells possess apical projections that sense luminal pH and release somatostatin when pH falls to <2 (104). Corpus D cells lack these projections and are insensitive to luminal pH changes (35). ENS neuropeptides and gastrin must stimulate D cells in the corpus to secrete somatostatin, which acts in a paracrine manner to inhibit ECL and parietal cell activity (90, 110).

Gastric protection. Gastric acid is corrosive to host cells; thus, to protect epithelia, bicarbonate ions are released into the mucus layer. Bicarbonate ions buffer secreted acid and increase pH at the mucus-epithelial interface to tolerable levels (78). Although gastric protection is important, it is not thoroughly described in our model, except to correct for acid levels buffered by bicarbonate ions (see APPENDIX).

Experiments

Parameter estimation. Once the model is developed and before simulations are performed, rates of each of the processes outlined in Figs. 1*B* and 3 must be estimated. Rate parameters are estimated from published experimental data and are presented in Table 1. Human-derived experimental data are used in estimations when possible. Animal data are used when no human data are available to derive magnitude estimates. In the absence of data, mathematical estimation is used. All parameters are evaluated using uncertainty analyses performed with C code based on Latin hypercube sampling (LHS) (9, 37, 38). To estimate cell population numbers, we perform immunohistochemistry on representative cross sections of human stomach mucosa (see below; see APPENDIX for details of parameter estimation).

Estimation of model parameters using animal data is hampered by species differences. For example, it is reported that there are significantly more ECL cells in rats than in humans (35) and that ECL cells comprise 66% of the endocrine cell population in the corpus in the rat (35) but only 30%

Table 1. *Parameters included in model analysis*

Parameter	Description	Value	Ref.	Unit
K_{NG_1}	Maximal secretion rate of gastrin due to ENS stimulation per cell	6.28×10^{-17}	12, 36, 73	$M\cdot h^{-1}\cdot cell^{-1}$
K_{NG_2}	Maximal secretion rate of gastrin due to CNS stimulation per cell	8.75×10^{-17}	68	$M\cdot h^{-1}\cdot cell^{-1}$
K_{PG}	Maximal secretion rate of gastrin due to ENS stimulation per cell	9.39×10^{-18}	*	$M\cdot h^{-1}\cdot cell^{-1}$
α_{NG_1}	Concn of ENS stimulant at which rate of gastrin secretion is 50%	1.0×10^{-10}	36	M
α_{NG_2}	Intensity of regulator at which rate of gastrin secretion is 50%	1.0×10^{-10}	36	M
k_{SG}	Dissociation constant of somatostatin from somatostatin receptor	9.0×10^{-11}	86	M
K_G	Clearance rate of gastrin	11.88	29	h^{-1}
β_G	Transport rate of gastrin from antrum to corpus region	1.5	*	h^{-1}
K_{AS}	Maximal rate of secretion of somatostatin due to stimulation with antrum acid	8.04×10^{-15}	*	$M\cdot h^{1}\cdot cell^{-1}$
K_{GS}	Maximal rate of secretion of corpal somatostatin due to stimulation with antral gastrin	2.54×10^{-18}	38	$M\cdot h^{-1}\cdot cell^{-1}$
α_{AS}	Acid concn at which rate of somatostatin secretion is half-maximal	0.05	63	M
α_{GS}	Gastrin concn at which rate of somatostatin secretion is half-maximal	5.20×10^{-12}	92	M
k_{NS}	Dissociation constant of GRP from receptors on D cells	1.0×10^{-9}	90	M
K_S	Clearance rate of somatostatin	13.86	33	h^{-1}
K_{NS_1}	Maximal rate of secretion of antral somatostatin due to enteric nervous stimulus	1.14×10^{-15}	36, 90	$M\cdot h^{-1}\cdot cell^{-1}$
K_{NS_2}	Maximal rate of secretion of corpal somatostatin due to enteric nervous stimulus	1.54×10^{-17}	90	$M\cdot h^{-1}\cdot cell^{-1}$
α_{NS_1}	Concn of ENS stimulant at which rate of antral somatostatin secretion is half-maximal	6.28×10^{-7}	*	M
α_{NS_2}	Concentration of ENS stimulant at which rate of corpal somatostatin secretion is half-maximal	8.98×10^{-11}	*	M
k_{SS}	Dissociation constant of somatostatin from somatostatin receptors on D cells	9.0×10^{-11}	86	M
K_{NH}	Maximal rate of histamine secretion due to ENS stimulation	7.59×10^{-16}	80	$M\cdot h^{-1}\cdot cell^{-1}$
K_{GH}	Maximal rate of histamine secretion stimulated by gastrin transported to corpal region	7.77×10^{-16}	1	$M\cdot h^{-1}\cdot cell^{-1}$
a_{NH}	Intensity of regulator at which rate of histamine secretion is half-maximal	3.25×10^{-8}	80	M
α_{GH}	Gastrin concn at which rate of histamine secretion is half-maximal	3.0×10^{-10}	1, 55, 60, 64, 82, 83	M
k_{SH}	Dissociation constant of somatostatin from somatostatin receptors on ECL cells	9.0×10^{-10}	86	M
K_H	Clearance rate of histamine	11.89	6	h^{-1}
K_{NA}	Maximal rate of acid secretion due to nervous stimulation mediated through ACh	2.33×10^{-11}	13	$M\cdot h^{-1}\cdot cell^{-1}$
K_{GA}	Maximal rate of acid secretion due to gastrin-mediated stimulation	4.98×10^{-11}	50	$M\cdot h^{-1}\cdot cell^{-1}$
K_{HA}	Maximal rate of acid secretion due to histamine-mediated stimulation	7.96×10^{-10}	50, 75	$M\cdot h^{-1}\cdot cell^{-1}$
α_{NA}	Concn CNS stimulant at which rate of acid output is half-maximal	5.0×10^{-6}	64, 75	M
α_{GA}	Gastrin concn at which rate of acid output is half-maximal	1.8×10^{-10}	84, 85	M
α_{HA}	Histamine concn at which rate of acid output is half-maximal	2.0×10^{-8}	64, 75	M
k_{SA}	Dissociation constant of somatostatin from somatostatin receptors on parietal cells	9.0×10^{-10}	86	M
β_A	Transfer rate of acid from corpus to antral region	2.72	*	h^{-1}
K_A	Washout rate of acid	2.72	53, 105	h^{-1}

ENS, enteric nervous system; CNS, central nervous system; concn, concentration; GRP, gastrin-releasing peptide; ECL, enterochromaffin-like. *Use of uncertainty analysis for parameter estimation.

in humans (15). These species differences are not limited to cells but are also observed at the level of effectors. Even given these difficulties, we find that estimating ranges for some parameters on the basis of order-of-magnitude estimates from animal studies yields results that are biologically feasible.

Uncertainty and sensitivity analyses. There are variances in many of the parameter values due to extensive variability in data. Such variances require an evaluation of the uncertainty in the system. We employ the LHS method to assess effects of uncertainties in our parameter estimation on model outcomes. LHS allows for simultaneous random, evenly distributed sampling of each parameter within a defined range. A matrix consisting of m columns corresponding to the number of varied parameters and n rows for the number of simulations is generated; n solutions are generated that show uncertainty in model outcomes due to parameter variations. For our uncertainty analyses, we run 20 short-term simulations (18 degrees of freedom; 24 h) varying a given parameter by a factor of 1,000. This is repeated for each parameter in the system individually and in combination.

By combining the uncertainty analyses outlined above with partial rank correlation (PRC), we are able to assess the sensitivity of our outcome variable (acid secretion) to parameter variation. This allows us to identify and quantify critical parameters (neural and nonneural) that dramatically affect the outcome when varied. In each case, a Student's t-test is used.

Immunohistochemistry. We obtained archived cross-sectional, biopsy, or surgical specimens of human stomach mucosa from individuals participating in a study on *Helicobacter pylori* colonization (University of Michigan Institution Review Board IRBMED no. 1999-0708). Biopsies were obtained from healthy regions of the stomach, and samples were fixed in 4% paraformaldehyde-PBS and embedded in paraffin. Sections were deparaffinized through an alcohol series and permeabilized in 3% H_2O_2 and 100% ethanol. Nonspecific

binding sites were blocked with 20% goat serum-PBS and 0.1% Triton X-100 for 30 min before 2 h of incubation with a 1:200 dilution of rabbit anti-gastrin-releasing peptide (GRP) antibody specific for G cells or mouse anti-H^+-K^+-ATPase β-subunit antibody (Medical and Biological Laboratories) specific for parietal cells. We incubated the samples in a 1:500 dilution of secondary anti-rabbit or anti-mouse IgG antibody for 30 min to conjugate secondary antibodies and achieved visualization in avidin-biotin complexes using the Vectastain Elite ABC kit and diaminobenzidine for substrate (Vector Laboratories, Burlingame, CA). Sections were also counterstained with hematoxylin and eosin. The stained cross sections were morphometrically analyzed by random selection of fields from which averages of each gastric cell type per gland could be assessed.

We estimate cell population using morphometry and use the three-dimensional nature of the gastric gland to extrapolate the numbers of each cell type. The result of one of these studies is shown in Fig. 2*B*. There are four to eight parietal cells per cross section of gland ($n = 5$). Corpus glands have a depth of ~0.1 mm (31), and parietal cells are observed to occupy approximately two-thirds of the glands, with an apical height of ~10 μm per cell. Given these dimensional data, we multiply the number of parietal cells per cross section of gland by a factor of 6. We estimate that there are 25–50 parietal cells per gland. In addition, there are $14–35 \times 10^6$ glands in the whole stomach, of which 75% are found in the corpus (25, 31). Therefore, we estimate that the number of parietal cells in the whole stomach ranges from 2.6×10^8 to 1.32×10^9, which is consistent with published morphometric data (Table 2). The number of D cells in the corpus is estimated by using similar methods.

We use a different procedure to estimate the number of antral G and D cells. From microscopic analysis of the antrum, we estimate that there are an average of 3.9 G cells ($n = 9$ glands) and 1.6 D cells ($n = 9$ glands) per antral gland. The G cell-to-D cell ratio obtained from our immunohistochemistry analysis is similar to G cell-to-D cell ratios reported previously (26). Experimental evidence suggests that there are <10 of each endocrine cell type per gastric gland (26, 77); therefore, the three-dimensional analysis used to estimate corpus D and parietal cells is not needed to estimate the numbers of antral cells. To deduce the number of G and D cells in the antrum, we assume that the antrum comprises 25% of the stomach, and, given the total number of gastric glands in the stomach (31), we calculate the number of each of the antral cell types (Table 1).

Computer simulations. Once we define the model and estimate parameters, we solve the system of ordinary differential equations (ODEs) to obtain temporal dynamics for each variable in our model. To this end, we use appropriate numerical methods for solving the system of ODEs over 24-h (short-term) and 5-day (long-term) periods. We use MatLab's ode15s solver for stiff systems (Math Works, Natick, MA) and compare results with those generated from a numerical algorithm using C code of a stiff adaptive solver based on the method of Rosenbrock and Storey (87) for consistency. Simulation results are also compared with similar experimental data.

Virtual depletions. To further validate our model, we perform virtual depletion experiments of different effectors of gastric acid secretion. We define our simulations as depletion experiments, because we set the appropriate variables (effectors) to be depleted to zero over a specific time frame. The system begins in steady state with wild-type conditions before depletion. An example of a depletion experiment involves neutralization of somatostatin. In contrast, in deletion experiments, a gene is disrupted or deleted; thus the system starts in a condition different from wild type. Virtual depletions are performed for gastrin, histamine, and somatostatin by using numerical methods and initial conditions (see above). We compare our results with published experimental depletion and deletion data. We then demonstrate the application of the model to address questions that are not easily addressed experimentally. For example, we independently deplete somatostatin in the corpus and antrum regions. Student's *t*-tests are used to evaluate significant differences between our virtual depletion simulations and appropriate controls.

Virtual ECL cell proliferation. To assess the role of gastrin in ECL cell proliferation, we induce prolonged hypergastrinemia (5 days) by increasing the maximal gastrin secretion rate due to CNS stimulation (K_{NG_1}). The three curves are each fitted to a generic quadratic form (e.g., $y = c + a_1t + a_2t^2$, where y represents the number of ECL cells, c and t are the initial number of ECL cells and time, respectively, and a_1 and a_2 are parameters that we estimated). Because the confidence intervals for the three curves do not overlap, their trajectories are significantly different.

RESULTS

We perform simulations that can be divided into two categories: *1*) those designed to validate the model and *2*) those that assess the importance of gastrin. We conduct simulations under normal conditions, and these serve as controls for subsequent simulated experiments. Simulations are performed over short-term (24-h) and long-term (5-day) time scales. Unless otherwise specified, we use the parameter values listed in Table 1. We first present baseline simulations compar-

Table 2. *Comparison of results obtained through immunohistochemical experiments and published data*

Cell Type	Steady-State Simulated Cell Numbers	Cells/Stomach	
		Immunohistochemistry estimates	Published data
G cells	8.75×10^6	$23.82 \times 10^6 \pm 14.44 \times 10^6$	$8.0–15 \times 10^6$ (88) 15.5×10^6 (dogs) (74) 16.6×10^6 (dogs) (100)
Antral D cells	3.70×10^6	$9.53 \times 10^6 \pm 5.77 \times 10^6$	G cell-to-D-cell ratio 2:1 (99) 11×10^6 (dogs) (74)
ECL cells	8.68×10^8	NA	30% total endocrine cell population (humans) (15, 32) 35% (97) 8.81×10^6 (rats)
Corpus D cells	2.69×10^8	$2.61 \times 10^8 \pm 0.83 \times 10^8$	4×10^6 (dogs) (74)
Parietal cells	1.00×10^8	$1.09 \times 10^9 \pm 2.4 \times 10^8$	1.005×10^9 (humans) (71)

NA, not assessed.

ing our results with published data and subsequently perform a series of virtual depletion experiments. Our simulation results represent effector levels in the extracellular spaces of the stomach mucosa. Experimentally, effector levels are typically determined from blood plasma measurements. Thus, in some cases, our simulation values are larger than those from published data and are accounted for by compartmental differences.

Baseline Conditions

Under normal conditions, we observe increases in neural and effector activity with food intake, which is consistent with experimental data (Fig. 5). The trimodal pattern of the feeding function (Fig. 4) is strongly correlated with neural and effector activity (Fig. 5). Food ingestion promotes release of gastrin, which is transported to the corpus. This transport implies a delay between the release of gastrin and its stimulatory effects. We are able to observe this delay between gastrin and histamine release using this model (data not shown), and we have developed a separate study exploring this delay (unpublished observations). In addition, the model also reproduces a characteristic reciprocal behavior of gastrin and antral somatostatin that is observed in in vivo and in vitro systems (Fig. 5*J*; cf. Ref. 110). This highlights the antagonistic relationship between the two effectors: gastrin release occurs first, followed by somatostatin activity, which downregulates gastrin secretion.

Cell population sizes remain consistent over 24 h (Fig. 6), and this finding is consistent with biological evidence (62). Although cell numbers are in homeostasis during the short term, we capture changes in cell numbers in the long term (data not shown), and we show cell dynamics under altered conditions (see below).

Virtual Depletion Experiments

To further validate the model as well as identify key effectors, we perform several depletion studies and compare results with experimental data. In each vir-

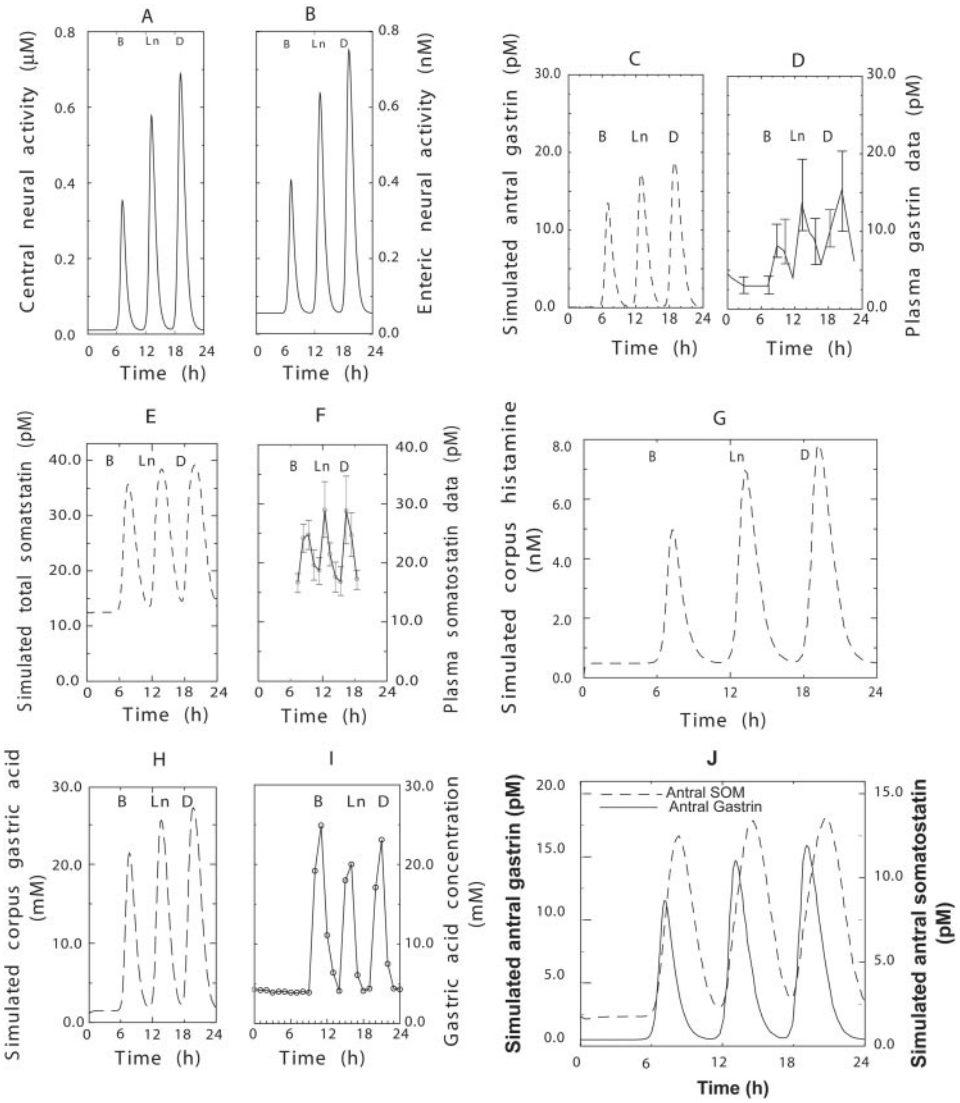

Fig. 5. Baseline simulations of effectors and gastric acid. *A*: simulation of CNS activity. *B*: simulation of ENS activity. *C*: virtual simulation of changes in plasma gastrin concentration due to release of gastrin by G cells. *D*: simulated gastrin release is in agreement with published plasma data (98). Upper and lower bounds of gastrin concentration are shown. *E*: simulated total somatostatin released by antral and corpus D cells. *F*: simulated somatostatin release (*E*) is consistent with experimental results (10). *G*: simulated histamine release from ECL cells. No human data on histamine diurnal changes have been reported. *H*: simulated gastric acid in corpus is consistent with experimental data from Feldman and Richardson (21) (*I*) showing upper and lower bounds of gastric acid. *J*: reciprocal behavior of gastrin and somatostatin (SOM) at 0700, 1300, and 1900.

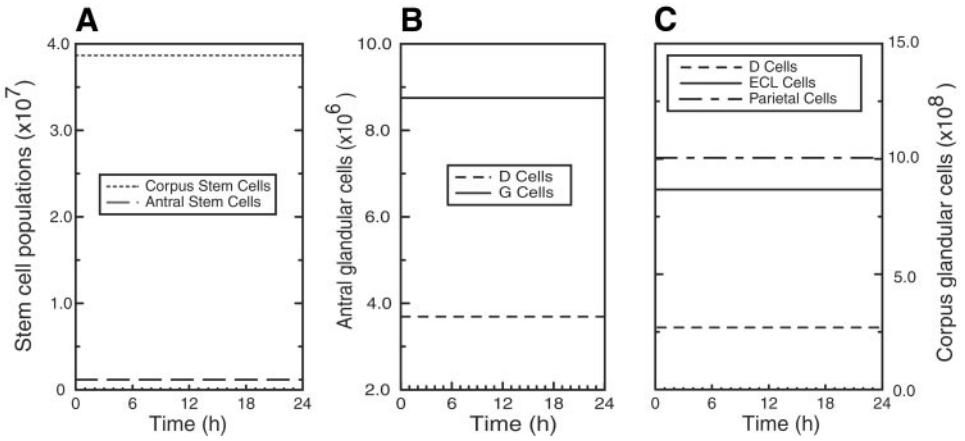

Fig. 6. Simulated cell populations. Cell population numbers remain in homeostasis over the 24-h time course. *A*: stem cells in corpus and antrum. *B*: antral endocrine cells include G and D cells. *C*: cells in corpus include D, ECL, and parietal cells.

tual depletion experiment, the depleted variable remains at zero during the 24-h simulation.

Gastrin depletion. Consistent with published data, we show a significant reduction of basal and stimulated acid secretion ($P < 0.001$; Fig. 7) (24, 34, 106). We suggest that this reduction is due to a decline in the secretion of downstream effectors (Fig. 7). In the long term, we also observe a decline in ECL cell populations that is consistent with similar experimental observations (24) (data not shown). This indicates a critical role for gastrin in maintenance of cell homeostasis.

Histamine depletion. During histamine depletion, we observe a significant reduction in acid levels ($P < 0.001$; Fig. 8), in agreement with experimental data (51). This reduced output is less dramatic than that observed during gastrin depletion (Fig. 7). Consistent with previously published data (51), basal acid levels are unaffected (Fig. 8). Gastrin is significantly elevated by 25% over wild-type conditions ($P < 0.001$). This is not as significant as the 300% increase in gastrin reported in mice with dysfunctional histamine receptors (51); however, this discrepancy is likely due to species-specific differences. In mice with deleted histamine receptors, acid secretion stimulated by gastrin is eliminated (51). On the contrary, in human studies using histamine antagonists, gastrin stimulates parietal cells to release acid (56). Hypergastrinemia continues during the duration of histamine depletion, resulting in a slow ECL cell overgrowth (data not shown).

Somatostatin depletion. Simulated basal effector levels are higher during somatostatin depletion than during control simulations ($P < 0.001$; data not shown).

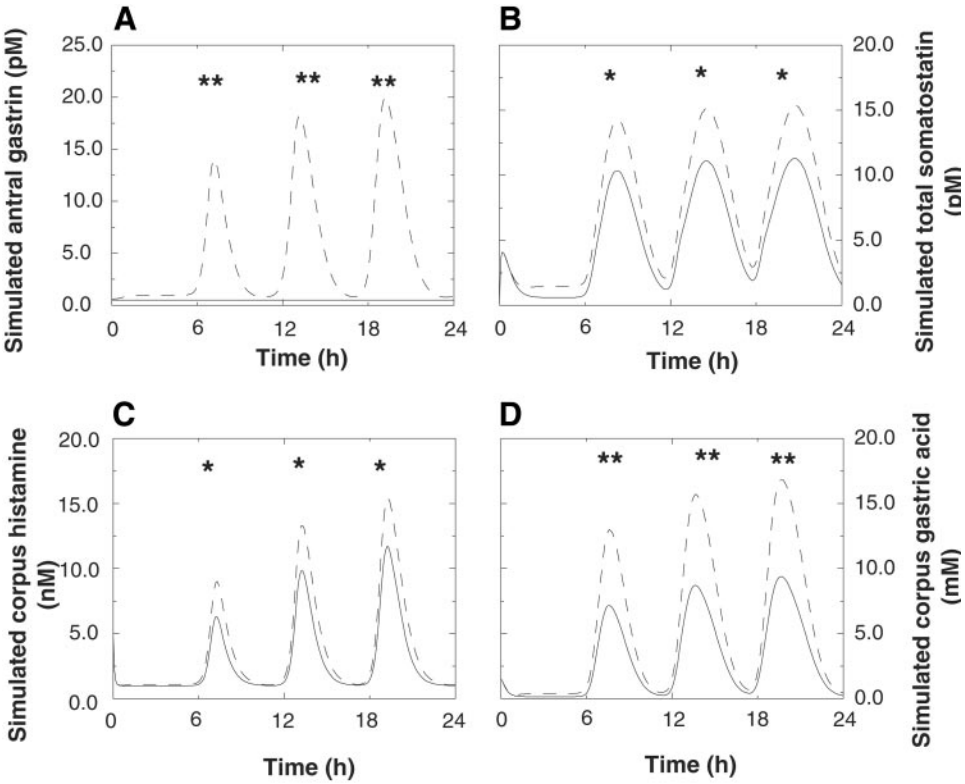

Fig. 7. Virtual depletion of gastrin. *A*: simulated gastrin. *B*: during gastrin depletion, somatostatin levels are lowered. *C* and *D*: histamine levels are reduced because of lack of gastrin stimulation and levels of gastric acid, respectively. Dashed lines, control; solid lines, histamine depletion. *$P < 0.05$; **$P < 0.001$.

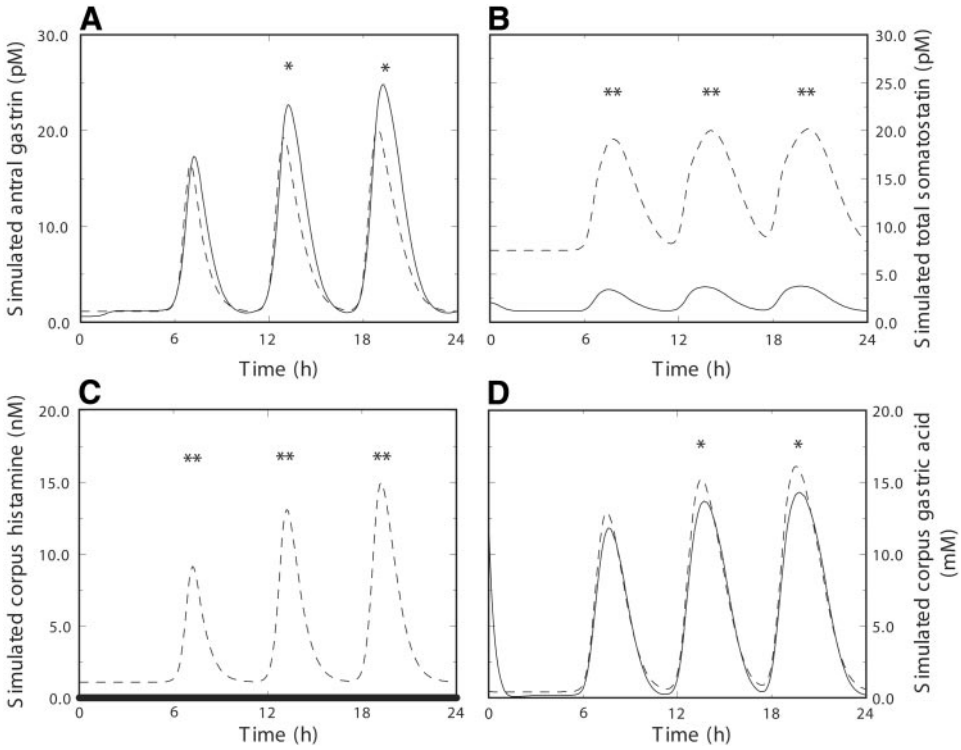

Fig. 8. Virtual histamine depletion. During histamine depletion, gastrin is elevated (*A*) and somatostatin concentration is significantly reduced (*B*). *C*: simulated histamine levels. *D*: lack of histamine significantly reduces gastric acid levels, although to a lesser extent than during gastrin depletion. Dashed lines, control; solid lines, histamine depletion. $^{*}P < 0.05$; $^{**}P < 0.001$.

This is in agreement with data demonstrating the inhibitory role of somatostatin in regulating intragastric acidity using somatostatin receptor subtype 2 (sst-2)-deficient mice (66). We also observe increases in stimulated secretion of effectors inhibited by somatostatin. Histamine levels significantly increase by 15% ($P < 0.001$; data not shown), and gastrin levels are slightly elevated by 2.5%.

Antral vs. corpus somatostatin depletion. Of key interest is the difference between the contribution of somatostatin from the antral region and that from the corpus region. Using our human model of gastric acid secretion, we are able to preferentially deplete somatostatin in either region, an experiment that is impossible to perform. Given the known dissimilarities between antral and corpus D cells (see above), we expect the impact of antral and corpus somatostatin on system dynamics to differ significantly. Gastrin is significantly elevated by 15% during antral somatostatin depletion ($P < 0.05$), whereas it is unchanged during corpus somatostatin depletion (Fig. 9). Histamine levels are significantly increased (900%) during antral somatostatin depletion compared with corpus somatostatin depletion (7%). Our results indicate that antral somatostatin depletion has a much greater effect on acid output than somatostatin produced in the corpus.

Effect of Food

There is a clear correlation between the feeding function (Fig. 4) and effector and acid levels (Fig. 5). To study this dependence, we supply various feeding functions whereby we vary the intervals between meals, the volume of food consumed, and the number of meals provided each day. In each case, the system response is directly correlated with the pattern of the feeding function. A stability analysis reveals stable limit cycles with periods that correspond to the modality of the feeding function (data not shown, unpublished observations).

Importance of the CNS

Using uncertainty and sensitivity analyses, we are able to assess the importance of each parameter, individually and in combination, on the dynamics of acid secretion. Rates governing CNS activity have the greatest effects on the system when varied (Fig. 10, *A* and *B*). Variations in CNS activity due to food stimulation have dramatic effects on our outcome variable, gastric acid (PRC coefficient = 0.94, $P \ll 0.001$). This is not surprising given the direct proportionality between CNS activity and food stimulus. We also observe that variations in food input propagate via the CNS throughout the system (data not shown; see above). Surprisingly, variations in the maximal gastrin secretion rate due to CNS stimulation (range 6.28×10^{-20}–6.28×10^{-17} $M \cdot h^{-1} \cdot cell^{-1}$) do not have significant effects on acid levels ($P > 0.5$). We observe reductions in acid secretion when the maximal rate of gastrin secretion due to CNS stimulation is significantly increased (Fig. 10, *C* and *D*).

Importance of Neural-Independent Parameters

We also identify parameters independent of neural activity that have significant effects on gastric acidity. Variations in the transport rate of gastrin between the antral and corpus regions exert the strongest effect on

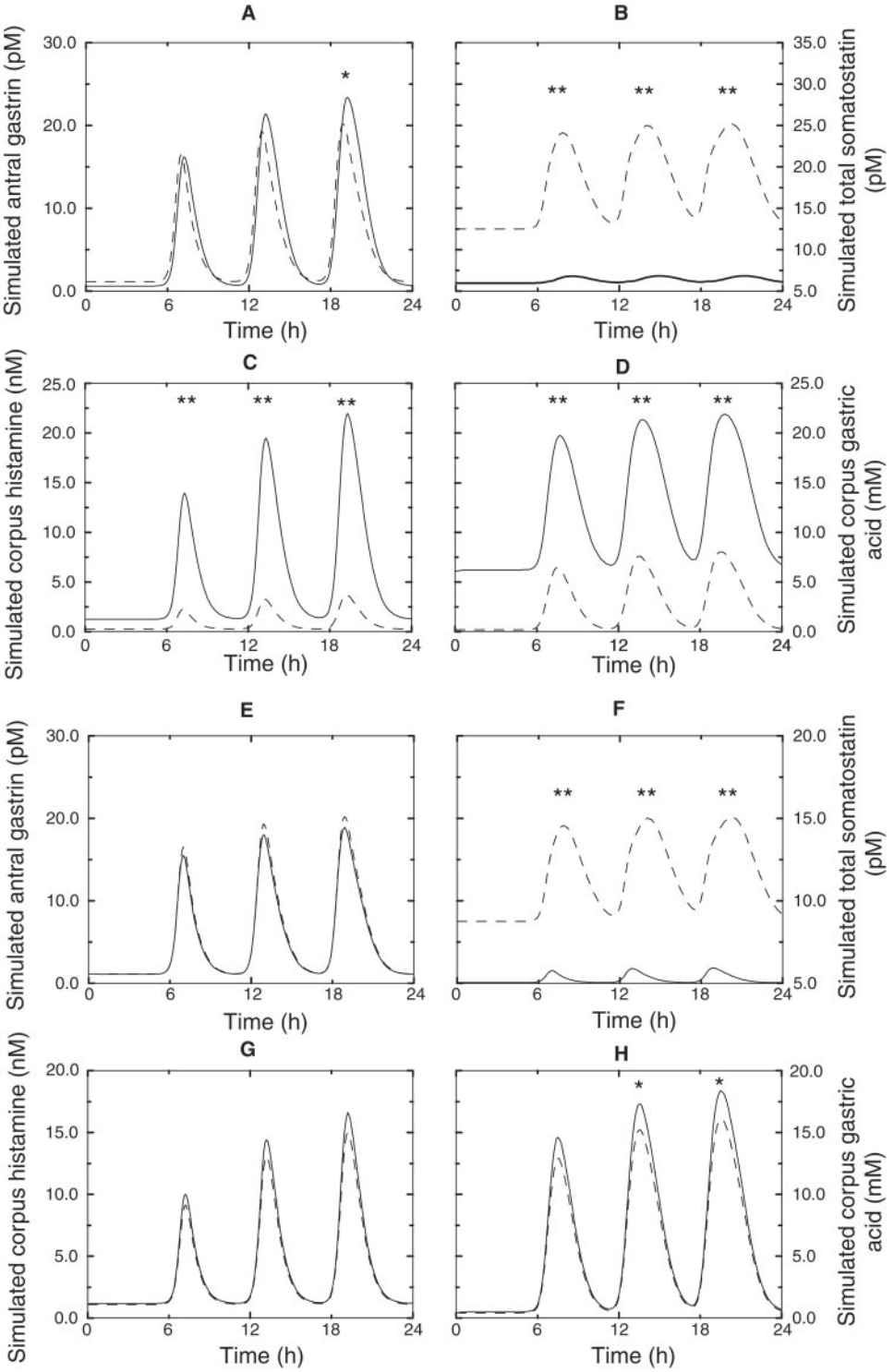

Fig. 9. Virtual depletion of somatostatin in antrum (*A–D*) and corpus (*E–H*). Antral somatostatin depletion has a more dramatic effect on the gastric system than does corpus somatostatin depletion. Breakfast, lunch, and dinner were provided at 0700, 1300, and 1900, respectively. Dashed lines, control; solid lines, histamine depletion. $^{*}P < 0.05$; $^{**}P < 0.001$.

acid levels (PRC coefficient = 0.80, $P \ll 0.001$). This is not unexpected given evidence for increased mucosal blood flow during feeding (49, 69, 79). We suggest that increasing blood flow increases the availability of gastrin in the corpus, thereby enhancing acid release. Although gastrin is important in acid secretion, we cannot omit the significance of the negative feedback of somatostatin. Not surprisingly, we observe a variety of somatostatin-associated parameters that also exert significant effects on acid release. These parameters include dissociation constants of somatostatin from G and ECL cell receptors ($P \ll 0.001$ for both parameters) as well as the maximal somatostatin secretion rate stimulated by luminal acid ($P < 0.05$). In the case of dissociation constants, somatostatin dissociation from receptors on G cells exerts a stronger effect than

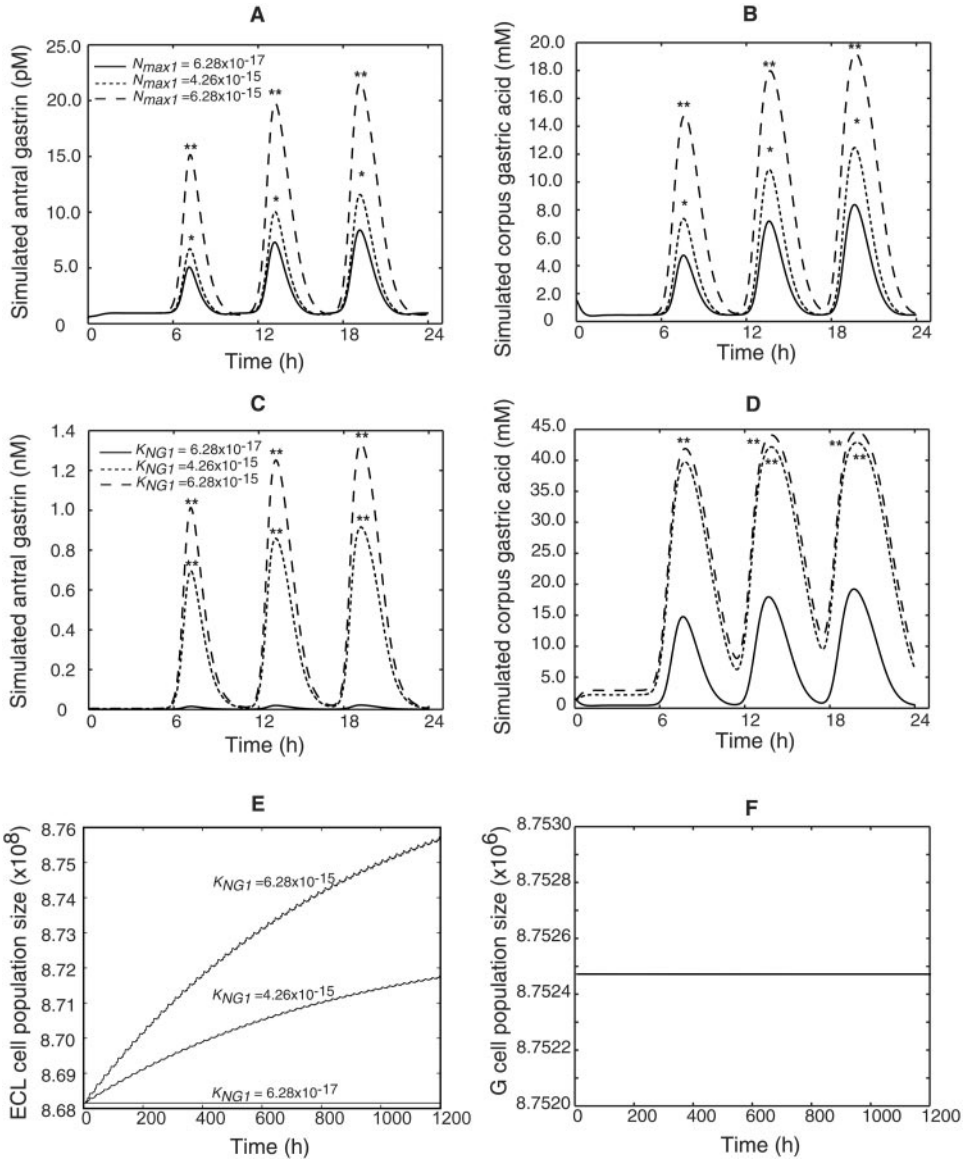

Fig. 10. Effect of variation of CNS parameters. *A* and *B*: effects of variation of maximal CNS activity due to food stimulation ($N_{\max_1}$) on simulated gastrin and gastric acid, respectively. *C* and *D*: effects of variation of maximal gastrin secretion rate due to CNS stimulation (K_{NG_1}) on simulated antral gastrin and gastric acid, respectively. *E*: long-term effects of gastrin on ECL overgrowth over 1,200 h (5 days). Gastrin levels are elevated after increases in maximal gastrin secretion rate due to CNS stimulation (K_{NG_1}). *F*: long-term effects of gastrin on G cells over 1,200 h (5 days). There is no change in G cell population as K_{NG_1} increases. $^*P < 0.05$; $^{**}P < 0.001$.

its dissociation from ECL cell receptors. This agrees with our comparison of antral and corpus somatostatin depletion (Fig. 9), in which we show the stronger effect of antral than of corpus somatostatin on acid release.

Effect of Gastrin on ECL Cell Growth

Using our mathematical model, we investigate the role of gastrin in ECL cell proliferation (Fig. 10*E*). When we increase gastrin levels by increasing the maximal gastrin secretion rate due to CNS stimulation (Fig. 10, *C* and *D*), ECL cell proliferation increases (Fig. 10*E*), whereas proliferation of other cells does not (Fig. 10*F*). We use nonlinear parameter estimation of a generic quadratic form to assess the significance of each ECL cell increase and demonstrate that their respective 95% confidence intervals do not overlap (data not shown). This suggests that induced ECL cell proliferation is significant. Our results are consistent with in vivo data where only long-term administration of proton pump inhibitors (112) or blockade of histamine-2 receptors (52) promotes ECL cell overgrowth.

DISCUSSION

We present a model of human gastric acid secretion using a system of 18 nonlinear ODEs together with a food function. In this system, positive and negative effectors strictly maintain acid homeostasis, the degree of which depends on food input. We show that the model is valid by demonstrating consistency with experimental results under normal and depletion conditions. The key modulators of the system are food and neural input. We also demonstrate the significance of gastrin through depletion studies. This is further substantiated by using sensitivity analyses, and together these findings suggest that gastrin is an important signal transducer relaying information from the CNS to parietal cells. We also demonstrate that although gastrin is important, somatostatin activity is a key regulator of gastric acidity.

Maintenance of gastric acid levels is important for optimal function of the stomach (28). Food digestion and sterilization of the lumen require strict control of acid levels, implying that the system returns quickly to equilibrium if disturbed. We find that our model satisfies this requirement, thereby suggesting that the gastric system is stable. Although redundancies ensure that gastric acid release continues if one pathway is lost, these redundancies cannot fully explain gastric stability. Maintenance of stability requires extensive feedback mechanisms that act to achieve homeostasis during disturbances. We show that compensatory mechanisms are likely invoked to stabilize acid secretion during altered conditions, such as effector depletion.

During virtual depletion of histamine, we observe a compensatory mechanism whereby the D cell population declines, promoting elevation of gastrin levels by reducing somatostatin production. When gastrin levels rise, gastric acid secretion is stimulated. This may account for the higher acid levels during histamine depletion (Fig. 8*D*) than during gastrin depletion (Fig. 7*D*). During virtual gastrin depletion, gastric acid secretion is reduced. We argue that, by boosting ECL cell numbers, histamine levels would increase, thereby restoring acid levels. On the contrary, this is not observed in gastrin knockout mice (34, 106). We therefore suggest that gastrin, and not histamine, plays a pivotal compensatory role. Furthermore, we suggest that gastrin levels may be useful as indicators of gastric health status.

We also demonstrate the significance of the negative-feedback loop involving somatostatin in acid release. Therefore, intact negative regulation is critical for proper function of the gastric system. We demonstrate that acid levels are sensitive to variations in somatostatin dissociation from G and ECL cells. Variations in these parameters may have dramatic and even detrimental effects on acid secretion given the prominence of somatostatin in inhibition of acid release. This may partially explain why these parameters do not vary significantly unless manipulated experimentally (108). Although somatostatin is important in inhibition of acid, it may also play a compensatory role controlling gastrin levels, thereby modulating acid secretion. During long-term absence of somatostatin, higher gastrin levels may promote ECL cell overgrowth. On the other hand, chronic elevations in somatostatin levels lower gastrin levels and may lead to loss of mucosal integrity. Therefore, we suggest that somatostatin levels are strictly controlled to maintain acid and cell homeostasis.

We demonstrate a technique for exploring gastric acid secretion and its regulation by gastric effectors. Mathematical models are not only applicable to long- and short-term studies, but they allow for rapid assessment of global effects. We are able to quickly assess critical elements in the system using virtual depletion/deletion analyses. Although our model is a simplification of human gastric acid secretion and its regulation, we include cells and effectors that are conserved among different species. Species-specific differences do not significantly affect our results, because we capture qualitatively and, to some extent, quantitatively the dynamical behavior of the human system.

Our model is a powerful tool for analyzing gastric effector and acid secretion, but there are limits to its potential. One of our immediate goals is to model acid secretion to assess important effectors in the system. To do this, we neglect many of the complex cellular events that contribute to the secretion of effectors and acid. Therefore, we cannot precisely reproduce some of the dynamical behaviors in secretion that are observed experimentally. For example, the secretion of somatostatin is biphasic, and this may be due to intracellular calcium release, which is intimately coupled to somatostatin release (18). We also observe differences in some of the cell dynamics compared with in vivo and in vitro data. We attribute these discrepancies, such as the elevation of immature cell populations, to model simplifications. In the case of cell dynamics, we do not account for intermediate cell stages observed during stem cell differentiation. Although cell and signal transduction dynamics are not modeled rigorously, this does not detract from the qualitative significance of our results. Inclusion of some of these events may render the model too complex for study.

Although the main purpose of the stomach is food digestion, pathogens can be ingested with food. Many of these pathogens are acid intolerant; thus acid secretion mechanisms help maintain a sterile environment. However, *H. pylori* has adapted to persist in this hostile environment. Most infections are asymptomatic and persist for the lifetime of the host; other outcomes such as peptic ulcer and gastric carcinomas occur less often. One key application of this model is to study colonization by this pathogen. For example, one effect of bacterial colonization is a significant elevation of gastrin levels (101, 111), the significance of which is not fully understood. Recent studies in mice have demonstrated that this response is not specific to *H. pylori* but, rather, involves mixed flora that colonize the mouse stomach (111). It is therefore possible that elevated gastrin levels during colonization may be host induced and may represent an effort toward bacterial clearance by increasing gastric acidity. With this model, we have another tool for exploring not only host-bacterial interactions but also the potential importance of compensatory mechanisms in bacterial persistence.

Another model application is designing therapeutic strategies to diminish effects of gastric ailments associated with *H. pylori*. A recent study has suggested that prolonged use of proton pump inhibitors by individuals infected with cytotoxin-associated gene A-positive *H. pylori* strains accelerates progression of gastric mucosal atrophy (27). Furthermore, although they are effective in reducing acid output, long-term administration of proton pump inhibitors may predispose individuals with gastrinomas to ECL cell overgrowth (23). Our model could be used to identify targets for reducing acid secretion without harmful side effects.

APPENDIX

Life spans of gastric cells. Life spans of gastric cells vary from species to species, and data on life spans of cells are

scarce, so we use murine data (40, 43–46). Units for growth, differentiation, and death rates are reported per day, and we convert them to units of per hour. We find the model to be robust, in that parameters within the range of a factor of 1,000 do not dramatically affect the outcomes.

Parameters for factors that influence growth, differentiation, and death of cells. We assume that gastrin-mediated proliferation of cells follows Michaelis-Menten kinetics; thus we use uncertainty analyses to estimate maximal growth rates and half-maximal proliferation. Kinetic studies regarding influences of prolonged starvation on stomach physiology are not available; therefore, we estimate these parameters using sensitivity analyses. We assume that loss of cells due to starvation also occurs via Michaelis-Menten kinetics. We estimate the maximal loss of cells due to starvation (λFd_{max}) and a threshold at which cell loss is half-maximal (α_{Fd}).

Effector and acid parameters. Effector release dynamics can be described by Michaelis-Menten kinetics. In the absence of stimulus, effector secretion remains at basal levels; however, effector secretion is enhanced on stimulation at a rate that is approximately proportional to stimulus intensity. Subsequently, as stimulus intensity increases, a maximal rate of effector secretion is achieved. Again, we estimate maximal rates and half-maximal constants of effector and acid secretion on stimulation.

The parameters described above constitute parameters in the positive terms of the differential equations. For loss terms, degradation and transfer are incorporated. Degradation rates are estimated from the half-life of each effector. *Equation A1* is employed in the derivation of these degradation rates

$$\kappa = {}^{\ln 2}/_{\text{half-life}} \tag{A1}$$

Flow rates between corpus and antrum are estimated from experimental data. We assume that the flow of acid from the lumen of the corpus to the antrum (β_A) is in equilibrium with the washout rate of stomach contents (κ_A) into the duodenum. Gastric content washout can be described by exponential decay kinetics. We obtain the half-life of gastric contents, and we use it to estimate the washout rate.

Model equations. Stem cells in the antrum undergo differentiation at a rate T_{Asc} to terminally developed G and D cells (Fig. 3*A*). Similar terminology describes the differentiation of stem cells in the corpus region. In both regions, loss of stem cells occurs only through differentiation. We assume that the antral and corpus stem cells divide at rates γ_{Asc} and γ_{Csc}, respectively, and model division of stem cell populations using logistic growth with defined carrying capacities. We also account for the effect gastrin may have on corpus stem cell differentiation by including the term $g_{max}[Gtn_C(t)]^2/[Gtn_C(t)]^2 + \alpha^2_{Csc}$ into differential *Eq. A3*. The differential equations describing stem cell population dynamics are as follows

$$\frac{dAsc(t)}{dt} = (\gamma_{Asc})\,[Asc(t)][C_{Asc} - Asc(t)] - [p_G(t) + p_{D_A}(t)]\,T_{Asc}\,[Asc(t)] \tag{A2}$$

for antral stem cells and

$$\frac{dCsc(t)}{dt} = (\gamma_{Csc})\,[Csc(t)]\,[C_{Csc} - Csc(t)] + \left\{\frac{g_{max}[Gtn_C(t)]^2}{[Gtn_C(t)]^2 + \alpha^2_{Csc}}\right\}Csc(t) - [p_E(t) + p_{D_C}(t) + p_P(t)]\,T_{Csc}\,[Csc\,(t)] \tag{A3}$$

for corpus stem cells.

We adopt the exponential term described by Sato et al. (89) to describe feedback mechanisms that modulate stem cell differentiation. In *Eqs. A2* and *A3*, the feedback mechanisms are given by $p_{G_c}(t)$, $p_{D_A}(t)$, $p_E(t)$, $p_{D_C}(t)$, and $p_P(t)$ and have the general form

$$P_{N_i}(t) = e^{-f\cdot N(t)^2/N^{*2}}$$

where N represents the specific terminally differentiated cell type G, D_A, D_C, E, or P.

Stem cells differentiate to a specific cell type when the cell population falls below a critical value N^*; however, as the cell population increases above this critical value, differentiation ceases. Paracrine, endocrine, and parietal cells emerge from stem cells in their appropriate compartments. These cells undergo death at a rate λ specific to the cell type under study, completing the dynamic process. Death rates are exclusive of periodic sloughing of surface cells, which is known to occur every 3 days (30, 39, 76).

Starvation also effects a decrease in G cell numbers (93). We incorporate this feature into the model in the following form: $\lambda_{Fd_{max}}(1 - [Fd(t)]^2/\{[Fd(t)]^2 + \alpha^2_{Fd}\})$. As food intake is reduced, the rate of loss of G cells increases toward $\gamma_{Fd_{max}}$. In contrast, high acid levels simultaneously decrease G cell growth and promote antral D cell growth (3). In the case of G cells, we use $k_{g_{max}}[1 - ([A_C(t)]^2/\{[A_C(t)]^2 + \alpha^2_{H_A}\})]$. For antral D cells, we include the positive term $k_{d_{max}}[A_C(t)]^2/[A_C(t)]^2 + \alpha^2_{H_A}$ to capture the effect of acid on D cell growth.

We model the dynamics of paracrine, endocrine, and exocrine cells as follows

$$\frac{dG(t)}{dt} = p_G(t)\,T_{Asc}\,Asc(t) + k_{g_{max}}\left\{1 - \frac{[A_c(t)]^2}{[A_c(t)]^2 + \alpha^2_{H_A}}\right\} \times G(t) - \lambda_{Fd_{max}}\left\{1 - \frac{[Fd(t)]^2}{[Fd(t)]^2 + \alpha^2_{Fd}}\right\}G(t) - \lambda_{G_c}G(t) \tag{A4}$$

for G cells

$$\frac{dD_A(t)}{dt} = p_{D_A}(t)T_{Asc}\,Asc(t) + \left\{\frac{k_{d_{max}}\,[A_C\,(t)]^2}{[A_C(t)]^2 + \alpha^2_{H_A}}\right\} \times D(t) - \lambda_{D_A}\,D_A(t) + \lambda_{Fd_{max}}\left\{1 - \frac{[fd(t)]^2}{[fd(t)]^2 + \alpha^2_{Fd}}\right\}D_A(t) \tag{A5}$$

for antral D cells

$$\frac{dD_c(t)}{dt} = p_{D_C}(t)T_{Asc}Csc(t) - \lambda_{D_C}D_C(t) \tag{A6}$$

for corpus D cells

$$\frac{dE(t)}{dt} = p_E(t)T_{Csc}Csc(t) - \lambda_E E(t) + \left\{\frac{k_{E_{max}}[Gtn_c(t)]^2}{[Gtn_c(t)]^2 + \alpha^2_E}\right\}E(t) \tag{A7}$$

for ECL cells, and

$$\frac{dP(t)}{dt} = p_P(t)T_{Csc}Csc(t) - \lambda_P P(t) \tag{A8}$$

for parietal cells.

Effector regulation of acid secretion. We use Michaelis-Menten kinetics to describe effector secretion in response to stimuli. For example, gastrin secretion is dependent on CNS, ENS, and food stimuli in a dose-dependent manner. On the other hand, somatostatin acts in a noncompetitive manner (14). This result is incorporated into the Michaelis-Menten terms, because the noncompetitive inhibition of enzyme-catalyzed reactions has been extensively explored (14). Therefore, we include an inhibitory term of the general form 1 +

[I]/k, where [I] is inhibitor concentration. If two inhibitors exist, as in the case of inhibition of somatostatin secretion by somatostatin and the CNS neurotransmitter acetylcholine, we assume that the product of the inhibitory terms, $\{1 + [S(t)]/k_S\}\{1 + [N_c(t)]/k_N\}$, captures the desired inhibitory dynamics.

We propose that loss of gastrin from the antrum occurs via two mechanisms: transport and degradation. In both circumstances, we hypothesize that this loss is directly proportional to the gastrin concentration in the antrum ($[Gtn_A]$) at *time t*. We do not account for any other molecular mechanisms, such as active transport, that may affect gastrin transport into the blood circulatory network of the stomach, nor do we account for metabolic degradation. We suggest from our results that exclusion of these mechanisms, if they do exist, does not detract greatly from the qualitative outcome (data not shown).

The dynamics for effectors are defined by using the following equations

Gastrin, histamine, and central neural stimuli elicit the secretion of acid from parietal cells. Again, we employ Michaelis-Menten kinetics to describe stimulated acid secretion. Somatostatin acts noncompetitively to inhibit acid secretion. Loss of gastric acid from the corpus region occurs at a rate β_A. This acid passively diffuses to the antral region, where it reappears as the source term of the differential equation describing antral gastric acid (*Eq. A15*). Bicarbonate buffering of acid leads to further loss of acid. This is represented by a mass action term, $hb[A_C(t)][B_C(t)]$. In addition, we also describe the potentiation of histamine on gastrin-mediated gastric acid secretion using the following term: $[H_C(t)]/\{[H_C(t)] + \alpha_H\}$. This term multiplies the Michaelis-Menten term describing gastrin-stimulated acid secretion by parietal cells. Acid is lost through transportation, buffering, or washout. The equations for the rate of change of gastric acid in the corpus and antrum are as follows

$$\frac{d[Gtn_A(t)]}{dt} = G(t)\left(\frac{K_{NG_1}[N_E(t)]}{\{[N_E(t)] + \alpha_{NG_1}\}\left\{1 + \frac{[S_A(t)]}{k_{SG}}\right\}\left\{1 + \frac{[A_c(t)]^2}{[A_c(t)]^2 + k_{AG}^2}\right\}} + \frac{K_{NG_2}[N_C(t)]}{\{N_C(t)] + \alpha_{NG_2}\}\left\{1 + \frac{[S_A(t)]}{k_{SG}}\right\}\left\{1 + \frac{[A_C(t)]^2}{[A_C(t)]^2 + k_{AG}^2}\right\}} + \frac{K_{FG}[Fd(t)]}{\{[Fd(t)] + \alpha_{FG}\}\left\{1 + \frac{[S_A(t)]}{k_{SG}}\right\}\left\{1 + \frac{[A_C(t)]^2}{[A_C(t)]^2 + k_{AG}^2}\right\}}\right) - (k_G + \beta_G)[Gtn_A(t)] \quad (A9)$$

for antral gastrin

$$\frac{d[Gtn_C(t)]}{dt} = \beta_G[Gtn_A(t)] - \kappa_G[Gtn_C(t)] \quad (A10)$$

for corpus gastrin

$$\frac{d[S_A(t)]}{dt} = D_A(t)\left[\left(\frac{K_{AS}[A_A(t)]}{\{[A_A(t)] + \alpha_{AS}\}\left\{1 + \frac{[S_A(t)]}{k_{SS}}\right\}\left\{1 + \frac{[N_C(t)]}{k_{NS}}\right\}}\right) + \left(\frac{K_{GS}[N_E(t)]}{\{[N_E(t)] + \alpha_{NS}\}\left(1 + \frac{[S_A(t)]}{k_{SS}}\right)\left(1 + \frac{[N_C(t)]}{k_{NS}}\right)}\right)\right] - \kappa_S[S_A(t)] \quad (A11)$$

for antral somatostatin

$$\frac{d[S_C(t)]}{dt} = D_C(t)\left[\left(\frac{K_{NS}[N_E(t)]}{\{[N_E(t)] + \alpha_{NS}\}\left\{1 + \frac{[S_C(t)]}{k_{SS}}\right\}\left\{1 + \frac{[N_C(t)]}{k_{NS}}\right\}}\right) + \left(\frac{K_{GS}[Gtn_C(t)]}{\{[Gtn_C(t)] + \alpha_{GS}\}\left\{1 + \frac{[S_C(t)]}{k_{SS}}\right\}\left\{1 + \frac{[N_C(t)]}{k_{NS}}\right\}}\right)\right] - \kappa_s[S_C(t)] \quad (A12)$$

for corpus somatostatin

$$\frac{d[H_C(t)]}{dt} = E(t)\left[\left(\frac{K_{NH}[N_E(t)]}{\{[N_E(t)] + \alpha_{NH}\}\left\{1 + \frac{[S_C(t)]}{k_{SH}}\right\}}\right) + \left(\frac{K_{GH}[Gtn_C(t)]}{\{[Gtn_C(t)] + \alpha_{GH}\}\left\{1 + \frac{[S_C(t)]}{k_{SH}}\right\}}\right)\right] - \kappa_H[H_C(t)] \quad (A13)$$

for histamine

$$\frac{d[A_C(t)]}{dt} = P(t)\left[\left(\frac{K_{NA}[N_C(t)]}{\{[N_C(t)] + \alpha_{NA}\}\left\{1 + \frac{[S_C(t)]}{k_{SA}}\right\}}\right) + \left\{\frac{[H_C(t)]}{[H_C(t)] + \alpha_H}\right\}\left(\frac{K_{GA}[Gtn_C(t)]}{\{[Gtn_C(t)] + \alpha_{GA}\}\left\{1 + \frac{[S_C(t)]}{k_{SA}}\right\}}\right) + \left(\frac{K_{HA}[H_C(t)]}{\{[H_C(t)] + \alpha_{HA}\}\left\{1 + \frac{[S_C(t)]}{k_{SA}}\right\}}\right)\right] - hb[Ac(t)][Bc(t)] - \frac{k_{Fd_{max}}\,Fd(t)}{Fd(t) + \alpha_{FA}}[A_C(t)] - \beta_A[A_C(t)] \quad (A14)$$

for corpus gastric acid and

$$\frac{d[A_A(t)]}{dt} = \beta_A[A_C(t)] - \kappa_A[A_A(t)] \quad (A15)$$

for antral gastric acid.

Bicarbonate secretion follows Michaelis-Menten kinetics, with the CNS stimulating secretion. This secretion therefore reaches a maximum at CNS stimulus intensity considerably greater than the half-maximal threshold. Loss of free bicarbonate from the system occurs via buffering of acid, transport to the antrum from the corpus, or washout from the antrum to the intestines. Differential equations describing the change in bicarbonate concentration in the corpus and antrum are as follows

$$\frac{d[B_c(t)]}{dt} = \frac{k_{B_{c\,max}}[N_c(t)]}{[N_c(t)] + \alpha_{NB}} - hb[A_c(t)]\,[B_c(t)] - \beta_B[B_c(t)] \quad (A16)$$

for corpus bicarbonate and

$$\frac{d[B_A(t)]}{dt} = \frac{k_{B_{A\,max}}[N_c(t)]}{[N_c(t)] + \alpha_{NB}} - hb[A_A(t)][B_A(t)] - \kappa_B[B_A(t)] \quad (A17)$$

for antral bicarbonate.

The central and enteric neural stimuli, $[N_C(t)]$ and $[N_E(t)]$, respectively, are evoked by food stimulus $[Fd(t)]$. We assume that the qualitative behavior is adequately described by Michaelis-Menten kinetics; hence, the following differential equations define central and enteric neural activity, respectively

$$\frac{d[N_c(t)]}{dt} = \left(\frac{N_{max_1}Fd(t)}{[Fd(t) + k^1_{Fd}]\left\{1 + \frac{[A_c(t)]^2}{[A_c(t)]^2 + k^2_{AN_1}}\right\}}\right) - \kappa_{N_C}[N_C(t)] + Bas_1 \quad (A18)$$

$$\frac{d[N_E(t)]}{dt} = \left(\frac{N_{max_2}Fd(t)}{[Fd(t) + k^2_{Fd}]\left\{1 + \frac{[A_c(t)]^2}{[A_c(t)]^2 + k^2_{AN_2}}\right\}}\right) - \kappa_{N_E}[N_E(t)] + Bas_2 \quad (A19)$$

Feedback from the luminal acidic environment is accomplished by noncompetitive inhibition of neural activity and is represented by $1 + ([A_c(t)]^2/\{[A_c(t)]^2 + (k_{AN_1})^2\})$. In addition, we account for basal neural activity in the CNS and ENS in the form of Bas_1 and Bas_2, respectively.

We thank Drs. Linda Samuelson, Victor DiRita, Michael Savageau, Cary Engleberg, and David Gammack for helpful comments and Drs. Simeone Marino and Suman Ganguli for reviewing our model. Gastric biopsies were supplied by Drs. Nguyen Thuy Vinh, Nguyen N. Thanh, and Han van Mao (Center for Cancer Research, Hanoi, Vietnam).

This work is supported by National Heart, Lung, and Blood Institute Grant 1RO1 HL-62119.

REFERENCES

1. **Andersson N, Rhedin M, Peteri-Brunback B, Andersson K, and Cabero JL.** Gastrin effects on isolated rat enterochromaffin-like cells following long-term hypergastrinaemia in vivo. *Biochim Biophys Acta* 1451: 297–304, 1999.
2. **Arnold R, Hulst MV, Neuhof CH, Schwarting H, Becker HD, and Creutzfeldt W.** Antral gastrin-producing G-cells and somatostatin-producing D-cells in different states of gastric acid secretion. *Gut* 23: 285–291, 1982.
3. **Arnold R, Koop H, Nesslinger A, and Schwarting H.** Effect of drugs with acid-neutralizing and acid-suppressive effect on parietal cell function and on gastrin and somatostatin cell density of the stomach [in German]. *Z Gastroenterol* 21 *Suppl*: 104–110, 1983.
4. **Arnold R and Lankisch PG.** Somatostatin and the gastrointestinal tract. *Clin Gastroenterol* 9: 733–753, 1980.
5. **Bakke I, Qvigstad G, Sandvik AK, and Waldum HL.** The CCK-2 receptor is located on the ECL cell, but not on the parietal cell. *Scand J Gastroenterol* 36: 1128–1133, 2001.
6. **Belic A, Grabnar I, Karba R, Mrhar A, Irman-Florjanc T, and Primozic S.** Interdependence of histamine and methylhistamine kinetics: modelling and simulation approach. *Comput Biol Med* 29: 361–375, 1999.
7. **Bengtsson P, Lundqvist G, and Nilsson G.** Inhibition of acid formation and stimulation of somatostatin release by cholecystokinin-related peptides in rabbit gastric glands. *J Physiol* 419: 765–774, 1989.
8. **Bertrand P and Willems G.** Induction of antral gastrin cell proliferation by refeeding of rats after fasting. *Gastroenterology* 78: 918–924, 1980.
9. **Blower SM and Dowlatabadi H.** Sensitivity and uncertainty analysis of complex models of disease transmission: an HIV model, as an example. *Int Stat Rev* 62: 229–243, 1994.
10. **Burhol PG, Jorde R, Jenssen TG, Lygren I, and Florholmen J.** Diurnal profile of plasma somatostatin in man. *Acta Physiol Scand* 120: 67–70, 1984.
11. **Burns AJ and Le Douarin NM.** Enteric nervous system development: analysis of the selective developmental potentialities of vagal and sacral neural crest cells using quail-chick chimeras. *Anat Rec* 262: 16–28, 2001.
12. **Campos RV, Buchan AM, Meloche RM, Pederson RA, Kwok YN, and Coy DH.** Gastrin secretion from human antral G cells in culture. *Gastroenterology* 99: 36–44, 1990.
13. **Cantor P, Petersen MB, Christiansen J, and Rehfeld JF.** Does sulfation of gastrin influence gastric acid secretion in man? *Scand J Gastroenterol* 25: 739–745, 1990.
14. **Chew CS.** Inhibitory action of somatostatin on isolated gastric glands and parietal cells. *Am J Physiol Gastrointest Liver Physiol* 245: G221–G229, 1983.
15. **D'Adda T, Bertele A, Pilato FP, and Bordi C.** Quantitative electron microscopy of endocrine cells in oxyntic mucosa of normal human stomach. *Cell Tissue Res* 255: 41–48, 1989.
16. **Debas HT and Carvajal SH.** Vagal regulation of acid secretion and gastrin release. *Yale J Biol Med* 67: 145–151, 1994.

17. **De Beus AM, Fabry TL, and Lacker HM.** A gastric acid secretion model. *Biophys J* 65: 362–378, 1993.
18. **DelValle J, Wakasugi J, Takeda H, and Yamada T.** Linkage of $[Ca^{2+}]_i$ in single isolated D cells to somatostatin secretion induced by cholecystokinin. *Am J Physiol Gastrointest Liver Physiol* 270: G897–G901, 1996.
19. **Dockray GJ.** Gastrin and gastric epithelial physiology. *J Physiol* 518: 315–324, 1999.
20. **Engel E, Peskoff A, Kauffman GL Jr, and Grossman MI.** Analysis of hydrogen ion concentration in the gastric gel mucus layer. *Am J Physiol Gastrointest Liver Physiol* 247: G321–G338, 1984.
21. **Feldman M and Richardson CT.** Role of thought, sight, smell, and taste of food in the cephalic phase of gastric acid secretion in humans. *Gastroenterology* 90: 428–433, 1986.
22. **Ferri D and Liquori GE.** Ultrastructural identification of somatostatin-immunoreactive cells in the pyloric glands of the ruin lizard (*Podarcis sicula campestris* De Betta) by immunogold staining. *Gen Comp Endocrinol* 102: 370–376, 1996.
23. **Feurle GE.** Argyrophil cell hyperplasia and a carcinoid tumour in the stomach of a patient with sporadic Zollinger-Ellison syndrome. *Gut* 35: 275–277, 1994.
24. **Friis-Hansen L, Sundler F, Li Y, Gillespie PJ, Saunders TL, Greenson JK, Owyang C, Rehfeld JF, and Samuelson LC.** Impaired gastric acid secretion in gastrin-deficient mice. *Am J Physiol Gastrointest Liver Physiol* 274: G561–G568, 1998.
25. **Ghoshal NG and Bal HS.** Comparative morphology of the stomach of some laboratory mammals. *Lab Anim* 23: 21–29, 1989.
26. **Graham DY, Lew GM, and Lechago J.** Antral G-cell and D-cell numbers in *Helicobacter pylori* infection: effect of *H. pylori* eradication. *Gastroenterology* 104: 1655–1660, 1993.
27. **Gudlaugsdottir S, van Dekken H, Stijnen T, and Wilson JH.** Prolonged use of proton pump inhibitors, CagA status, and the outcome of *Helicobacter pylori* gastritis. *J Clin Gastroenterol* 34: 536–540, 2002.
28. **Guyton AC and Hall JE.** *Textbook of Medical Physiology*. Philadelphia, PA: Saunders, 2000.
29. **Hansen CP, Stadil F, Yucun L, and Rehfeld JF.** Pharmacokinetics and organ metabolism of carboxyamidated and glycine-extended gastrins in pigs. *Am J Physiol Gastrointest Liver Physiol* 271: G156–G163, 1996.
30. **Hattori T and Arizono N.** Cell kinetics and secretion of mucus in the gastrointestinal mucosa and their diurnal rhythm. *J Clin Gastroenterol* 10: S1–S6, 1988.
31. **Helander HF.** *The Stomach*, edited by Gustavsson S, Kumar D, and Graham DY. New York: Churchill Livingstone, 1992, p. 444.
32. **Helander HF, Rutgersson K, Helander KG, Pisegna JP, Gardner JD, Jensen RT, and Maton PN.** Stereologic investigations of human gastric mucosa. II. Oxyntic mucosa from patients with Zollinger-Ellison syndrome. *Scand J Gastroenterol* 27: 875–883, 1992.
33. **Hildebrand P, Ensinck JW, Buettiker J, Drewe J, Burckhardt B, Gyr K, and Beglinger C.** Circulating somatostatin-28 is not a physiologic regulator of gastric acid production in man. *Eur J Clin Invest* 24: 50–56, 1994.
34. **Hinkle KL and Samuelson LC.** Lessons from genetically engineered animal models. III. Lessons learned from gastrin gene deletion in mice. *Am J Physiol Gastrointest Liver Physiol* 277: G500–G505, 1999.
35. **Holst JJ.** The stomach as an endocrine organ. In: *Fernström Foundation Series*, edited by Håkanson R and Sundler F. New York: Elsevier, 1991, p. 548.
36. **Holst JJ, Knuhtsen S, Orskov C, Skak-Nielsen T, Poulsen SS, and Nielsen OV.** GRP-producing nerves control antral somatostatin and gastrin secretion in pigs. *Am J Physiol Gastrointest Liver Physiol* 253: G767–G774, 1987.
37. **Iman RL, Helton JC, and Campbell JE.** An approach to sensitivity analysis of computer models. I. Introduction, input variable selection and preliminary variable assessment. *J Qual Technol* 13: 174–183, 1981.
38. **Iman RL, Helton JC, and Campbell JE.** An approach to sensitivity analysis of computer models. II. Ranking of input variables, response surface validation, distribution effect and technique synopsis. *J Qual Technol* 13: 232–240, 1981.
39. **Inokuchi H, Fujimoto S, and Kawai K.** Cellular kinetics of gastrointestinal mucosa, with special reference to gut endocrine cells. *Arch Histol Jpn* 46: 137–157, 1983.
40. **Karam SM.** Dynamics of epithelial cells in the corpus of the mouse stomach. IV. Bidirectional migration of parietal cells ending in their gradual degeneration and loss. *Anat Rec* 236: 314–332, 1993.
41. **Karam SM.** New insights into the stem cells and the precursors of the gastric epithelium. *Nutrition* 11: 607–613, 1995.
42. **Karam S and Leblond CP.** Origin and migratory pathways of the eleven epithelial cell types present in the body of the mouse stomach. *Microsc Res Tech* 31: 193–214, 1995.
43. **Karam SM and Leblond CP.** Dynamics of epithelial cells in the corpus of the mouse stomach. I. Identification of proliferative cell types and pinpointing of the stem cell. *Anat Rec* 236: 259–279, 1993.
44. **Karam SM and Leblond CP.** Dynamics of epithelial cells in the corpus of the mouse stomach. II. Outward migration of pit cells. *Anat Rec* 236: 280–296, 1993.
45. **Karam SM and Leblond CP.** Dynamics of epithelial cells in the corpus of the mouse stomach. III. Inward migration of neck cells followed by progressive transformation into zymogenic cells. *Anat Rec* 236: 297–313, 1993.
46. **Karam SM and Leblond CP.** Dynamics of epithelial cells in the corpus of the mouse stomach. V. Behavior of entero-endocrine and caveolated cells: general conclusions on cell kinetics in the oxyntic epithelium. *Anat Rec* 236: 333–340, 1993.
47. **Karam SM and Leblond CP.** Identifying and counting epithelial cell types in the "corpus" of the mouse stomach. *Anat Rec* 232: 231–246, 1992.
48. **Kidd M, Modlin IM, and Tang LH.** Gastrin and the enterochromaffin-like cell: an acid update. *Dig Surg* 15: 209–217, 1998.
49. **Kiel JW, Riedel GL, and Shepherd AP.** Local control of canine gastric mucosal blood flow. *Gastroenterology* 93: 1041–1053, 1987.
50. **Kleveland PM, Waldum HL, and Larsson H.** Gastric acid secretion in the totally isolated, vascularly perfused rat stomach. A selective muscarinic-1 agent does, whereas gastrin does not, augment maximal histamine-stimulated acid secretion. *Scand J Gastroenterol* 22: 705–713, 1987.
51. **Kobayashi T, Tonai S, Ishihara Y, Koga R, Okabe S, and Watanabe T.** Abnormal functional and morphological regulation of the gastric mucosa in histamine H_2 receptor-deficient mice. *J Clin Invest* 105: 1741–1749, 2000.
52. **Kolby L, Wangberg B, Ahlman H, Modlin IM, Granerus G, Theodorsson E, and Nilsson O.** Histidine decarboxylase expression and histamine metabolism in gastric oxyntic mucosa during hypergastrinemia and carcinoid tumor formation. *Endocrinology* 137: 4435–4442, 1996.
53. **Kreiss C, Schwizer W, Borovicka J, Jansen JB, Bouloux C, Pignol R, Bischof Delaloye A, and Fried M.** Effect of lintitript, a new CCK-A receptor antagonist, on gastric emptying of a solid-liquid meal in humans. *Regul Pept* 74: 143–149, 1998.
54. **Lawton DE, Simcock DC, Candy EJ, and Simpson HV.** Gastrin secretion by ovine antral mucosa in vitro. *Comp Biochem Physiol A Mol Integr Physiol* 126: 233–243, 2000.
55. **Lawton GP, Tang LH, Miu K, Gilligan CJ, Absood A, and Modlin IM.** Adrenergic and cromolyn sodium modulation of ECL cell histamine secretion. *J Surg Res* 58: 96–104, 1995.
56. **Lazzaroni M, Ardizzone S, Imbimbo BP, Sangaletti O, Ghirardosi C, and Bianchi Porro G.** Effect of mifentidine, a new H_2-antagonist, on pentagastrin-stimulated acid secretion in healthy subjects. *Int J Clin Pharmacol Ther Toxicol* 25: 218–221, 1987.
57. **Licko V and Ekblad EB.** Dynamics of a metabolic system: what single-action agents reveal about acid secretion. *Am J Physiol Gastrointest Liver Physiol* 262: G581–G592, 1992.
58. **Licko V and Ekblad EB.** What dual-action agents reveal about acid secretion: a combined experimental and modeling analysis. *Biochim Biophys Acta* 1137: 19–28, 1992.

59. **Lindstrom E, Chen D, Norlen P, Andersson K, and Hakanson R.** Control of gastric acid secretion: the gastrin-ECL cell-parietal cell axis. *Comp Biochem Physiol A Mol Integr Physiol* 128: 505–514, 2001.
60. **Lindstrom E and Hakanson R.** Neurohormonal regulation of secretion from isolated rat stomach ECL cells: a critical reappraisal. *Regul Pept* 97: 169–180, 2001.
61. **Liquori GE, Ferri D, and Scillitani G.** Fine structure of the oxynticopeptic cells in the gastric glands of the ruin lizard, *Podarcis sicula campestris* De Betta, 1857. *J Morphol* 243: 167–171, 2000.
62. **Magami Y, Azuma T, Inokuchi H, Moriyasu F, Kawai K, and Hattori T.** Cell kinetics of slow renewing cell populations in mice stomach. *J Gastroenterol Hepatol* 17: 262–269, 2002.
63. **Makhlouf GM and Schubert ML.** Gastric somatostatin: a paracrine regulator of acid secretion. *Metabolism* 39: 138–142, 1990.
64. **Mardh S, Norberg L, Ljungstrom M, Wollert S, Nyren O, and Gustavsson S.** A method for in vitro studies on acid formation in human parietal cells. Stimulation by histamine, pentagastrin and carbachol. *Acta Physiol Scand* 123: 349–354, 1985.
66. **Martinez V, Curi AP, Torkian B, Schaeffer JM, Wilkinson HA, Walsh JH, and Tache Y.** High basal gastric acid secretion in somatostatin receptor subtype 2 knockout mice. *Gastroenterology* 114: 1125–1132, 1998.
67. **Marvik R, Sandvik AK, and Waldum HL.** Gastrin stimulates histamine release from the isolated pig stomach. *Scand J Gastroenterol* 32: 2–5, 1997.
68. **Matsuno M, Matsui T, Iwasaki A, and Arakawa Y.** Role of acetylcholine and gastrin-releasing peptide (GRP) in gastrin secretion. *J Gastroenterol* 32: 579–586, 1997.
69. **Mattsson H and Larsson H.** Effects of omeprazole on gastric mucosal blood flow in the conscious rat. *Scand J Gastroenterol* 22: 491–498, 1987.
70. **Murone M, Carpenter DA, and de Sauvage FJ.** Hematopoietic deficiencies in c-*mpl* and TPO knockout mice. *Stem Cells* 16: 1–6, 1998.
71. **Naik SR, Bajaj SC, Goyal RK, Gupta DN, and Chuttani HK.** Parietal cell mass in healthy human stomach. *Gastroenterology* 61: 682–685, 1971.
72. **Nederkoorn C, Smulders FT, and Jansen A.** Cephalic phase responses, craving and food intake in normal subjects. *Appetite* 35: 45–55, 2000.
73. **Nishi S, Seino Y, Takemura J, Ishida H, Seno M, Chiba T, Yanaihara C, Yanaihara N, and Imura H.** Vagal regulation of GRP, gastric somatostatin, and gastrin secretion in vitro. *Am J Physiol Endocrinol Metab* 248: E425–E431, 1985.
74. **Nomiyama S, Nishioka B, Ishii T, Nakamura K, and Majima S.** Comparative study of G- and D-cell population in the dog stomach. *Jpn J Surg* 11: 346–352, 1981.
75. **Norberg L, Ljungstrom M, Vega FV, and Mardh S.** Stimulation of acid formation by histamine, carbachol and pentagastrin in isolated pig parietal cells. *Acta Physiol Scand* 126: 385–390, 1986.
76. **Pansu D, Berard A, and Lambert R.** [Regulation of cell renewal in the gastrointestinal mucosa]. *Pathol Biol (Paris)* 25: 119–133, 1977.
77. **Park SM, Lee HR, Kim JG, Park JW, Jung G, Han SH, Cho JH, and Kim MK.** Effect of *Helicobacter pylori* infection on antral gastrin and somatostatin cells and on serum gastrin concentrations. *Korean J Intern Med* 14: 15–20, 1999.
78. **Phillipson M, Atuma C, Henriksnas J, and Holm L.** The importance of mucus layers and bicarbonate transport in preservation of gastric juxtamucosal pH. *Am J Physiol Gastrointest Liver Physiol* 282: G211–G219, 2002.
79. **Pique JM, Leung FW, Tan HW, Livingston E, Scremin OU, and Guth PH.** Gastric mucosal blood flow response to stimulation and inhibition of gastric acid secretion. *Gastroenterology* 95: 642–650, 1988.
80. **Pisegna JR, Ohning GV, Athmann C, Zeng N, Walsh JH, and Sachs G.** Role of PACAP1 receptor in regulation of ECL cells and gastric acid secretion by pituitary adenylate cyclase activating peptide. *Ann NY Acad Sci* 921: 233–241, 2000.
81. **Prinz C, Scott DR, Hurwitz D, Helander HF, and Sachs G.** Gastrin effects on isolated rat enterochromaffin-like cells in primary culture. *Am J Physiol Gastrointest Liver Physiol* 267: G663–G675, 1994.
82. **Prinz C, Zanner R, Gerhard M, Mahr S, Neumayer N, Hohne-Zell B, and Gratzl M.** The mechanism of histamine secretion from gastric enterochromaffin-like cells. *Am J Physiol Cell Physiol* 277: C845–C855, 1999.
83. **Roche S, Gusdinar T, Bali JP, and Magous R.** "Gastrin" and "CCK" receptors on histamine- and somatostatin-containing cells from rabbit fundic mucosa. II. Characterization by means of selective antagonists (L-364718 and L-365260). *Biochem Pharmacol* 42: 771–776, 1991.
84. **Roche S, Gusdinar T, Bali JP, and Magous R.** Biphasic kinetics of inositol 1,4,5-trisphosphate accumulation in gastrin-stimulated parietal cells. Effects of pertussis toxin and extracellular calcium. *FEBS Lett* 282: 147–151, 1991.
85. **Roche S, Gusdinar T, Bali JP, and Magous R.** Relationship between inositol 1,4,5-trisphosphate mass level and [^{14}C]aminopyrine uptake in gastrin-stimulated parietal cells. *Mol Cell Endocrinol* 77: 109–113, 1991.
86. **Rocheville M, Lange DC, Kumar U, Sasi R, Patel RC, and Patel YC.** Subtypes of the somatostatin receptor assemble as functional homo- and heterodimers. *J Biol Chem* 275: 7862–7869, 2000.
87. **Rosenbrock HH and Storey C.** *Mathematics of Dynamical Systems*. New York: Wiley Interscience, 1970.
88. **Royston CM, Polak J, Bloom SR, Cooke WM, Russell RC, Pearse AG, Spencer J, Welbourn RB, and Baron JH.** G cell population of the gastric antrum, plasma gastrin, and gastric acid secretion in patients with and without duodenal ulcer. *Gut* 19: 689–698, 1978.
89. **Sato F, Muramatsu S, Tsuchihashi S, Shiragai A, Hiraoka T, Inada T, Kawashima K, Matsuzawa H, Nakamura W, Trucco E, and Sacher GA.** Radiation effects on cell populations in the intestinal epithelium of mice and its theory. *Cell Tissue Kinet* 5: 227–235, 1972.
90. **Schaffer K, Herrmuth H, Mueller J, Coy DH, Wong HC, Walsh JH, Classen M, Schusdziarra V, and Schepp W.** Bombesin-like peptides stimulate somatostatin release from rat fundic D cells in primary culture. *Am J Physiol Gastrointest Liver Physiol* 273: G686–G695, 1997.
91. **Schubert ML, Bitar KN, and Makhlouf GM.** Regulation of gastrin and somatostatin secretion by cholinergic and noncholinergic intramural neurons. *Am J Physiol Gastrointest Liver Physiol* 243: G442–G447, 1982.
92. **Schubert ML, Edwards NF, Arimura A, and Makhlouf GM.** Paracrine regulation of gastric acid secretion by fundic somatostatin. *Am J Physiol Gastrointest Liver Physiol* 252: G485–G490, 1987.
93. **Schwarting H, Koop H, Gellert G, and Arnold R.** Effect of starvation on endocrine cells in the rat stomach. *Regul Pept* 14: 33–39, 1986.
94. **Schwartz GJ.** The role of gastrointestinal vagal afferents in the control of food intake: current prospects. *Nutrition* 16: 866–873, 2000.
95. **Schwartz GJ, Salorio CF, Skoglund C, and Moran TH.** Gut vagal afferent lesions increase meal size but do not block gastric preload-induced feeding suppression. *Am J Physiol Regul Integr Comp Physiol* 276: R1623–R1629, 1999.
96. **Shankley NP, Welsh NJ, and Black JW.** Histamine dependence of pentagastrin-stimulated gastric acid secretion in rats. *Yale J Biol Med* 65: 613–619, 1992.
97. **Simonsson M, Eriksson S, Hakanson R, Lind T, Lonroth H, Lundell L, O'Connor DT, and Sundler F.** Endocrine cells in the human oxyntic mucosa. A histochemical study. *Scand J Gastroenterol* 23: 1089–1099, 1988.
98. **Smith JT, Pounder RE, Nwokolo CU, Lanzon-Miller S, Evans DG, Graham DY, and Evans DJ Jr.** Inappropriate hypergastrinaemia in asymptomatic healthy subjects infected with *Helicobacter pylori*. *Gut* 31: 522–525, 1990.
99. **Solcia E, Capella C, Sessa F, Rindi G, Cornaggia M, Riva C, and Villani L.** Gastric carcinoids and related endocrine growths. *Digestion* 35: 3–22, 1986.

100. **Takahashi T, Shimazu H, Yamagishi T, and Tani M.** G-cell population in antral mucosa of the dog. *Dig Dis Sci* 24: 921–925, 1979.
101. **Testino G, Cornaggia M, and De Iaco F.** *Helicobacter pylori* influence on gastric acid secretion in duodenal ulcer patients diagnosed for the first time. *Panminerva Med* 44: 19–22, 2002.
102. **Tielemans Y, Axelson J, Sundler F, Willems G, and Hakanson R.** Serum gastrin concentration affects the self-replication rate of the enterochromaffin-like cells in the rat stomach. *Gut* 31: 274–278, 1990.
103. **Tielemans Y, Willems G, Sundler F, and Hakanson R.** Self-replication of enterochromaffin-like cells in the mouse stomach. *Digestion* 45: 138–146, 1990.
104. **Uvnas-Wallensten K, Efendic S, Johansson C, Sjodin L, and Cranwell PD.** Effect of intraluminal pH on the release of somatostatin and gastrin into antral, bulbar and ileal pouches of conscious dogs. *Acta Physiol Scand* 110: 391–400, 1980.
105. **Van Duijn B, Ypey DL, de Goede J, Verveen AA, and Hekkens W.** A model study of the regulation of gastric acid secretion. *Am J Physiol Gastrointest Liver Physiol* 257: G157–G168, 1989.
106. **Wang TC and Dockray GJ.** Lessons from genetically engineered animal models. I. Physiological studies with gastrin in transgenic mice. *Am J Physiol Gastrointest Liver Physiol* 277: G6–G11, 1999.
107. **Wollin A.** Regulation of gastric acid secretion at the cellular level. *Clin Invest Med* 10: 209–214, 1987.
108. **Yoshida K, Nishihara S, Misawa T, and Nawata H.** Somatostatin receptors and the effect of somatostatin on histamine-stimulated adenylate cyclase activity in isolated gastric glands of guinea pigs. *Gastroenterol Jpn* 24: 611–618, 1989.
109. **Zavros Y, Fleming WR, Hardy KJ, and Shulkes A.** Regulation of fundic and antral somatostatin secretion by CCK and gastrin. *Am J Physiol Gastrointest Liver Physiol* 274: G742–G750, 1998.
110. **Zavros Y, Fleming WR, and Shulkes A.** Concurrent elevation of fundic somatostatin prevents gastrin stimulation by GRP. *Am J Physiol Gastrointest Liver Physiol* 276: G21–G27, 1999.
111. **Zavros Y, Rieder G, Ferguson A, and Merchant JL.** Gastritis and hypergastrinemia due to *Acinetobacter lwoffii* in mice. *Infect Immun* 70: 2630–2639, 2002.
112. **Zhao CM, Bakke I, Tostrup-Skogaker N, Waldum HL, Hakanson R, and Chen D.** Functionally impaired, hypertrophic ECL cells accumulate vacuoles and lipofuscin bodies. An ultrastructural study of ECL cells isolated from hypergastrinemic rats. *Cell Tissue Res* 303: 415–422, 2001.